

CHEM MED CHEM

CHEMISTRY ENABLING DRUG DISCOVERY

Accepted Article

Title: Optimization of Pyrazoles as Phenol Surrogates to Yield Potent Inhibitors of Macrophage Migration Inhibitory Factor

Authors: Vinay Trivedi-Parmar, Michael J. Robertson, Jose A. Cisneros, Stefan G. Krimmer, and William L. Jorgensen

This manuscript has been accepted after peer review and appears as an Accepted Article online prior to editing, proofing, and formal publication of the final Version of Record (VoR). This work is currently citable by using the Digital Object Identifier (DOI) given below. The VoR will be published online in Early View as soon as possible and may be different to this Accepted Article as a result of editing. Readers should obtain the VoR from the journal website shown below when it is published to ensure accuracy of information. The authors are responsible for the content of this Accepted Article.

To be cited as: *ChemMedChem* 10.1002/cmdc.201800158

Link to VoR: <http://dx.doi.org/10.1002/cmdc.201800158>

WILEY-VCH

www.chemmedchem.org

A Journal of



COMMUNICATION

Optimization of Pyrazoles as Phenol Surrogates to Yield Potent Inhibitors of Macrophage Migration Inhibitory Factor

Vinay Trivedi-Parmar, Michael J. Robertson, José A. Cisneros, Stefan G. Krimmer, and William L. Jorgensen*

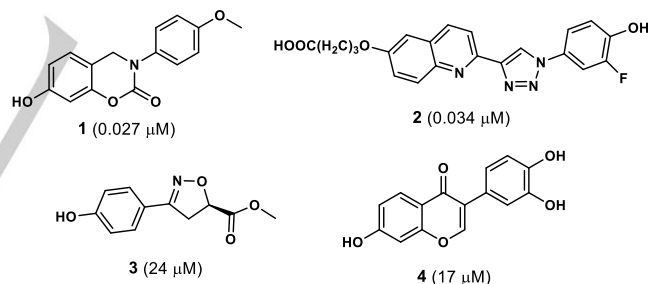
Dedicated to Prof. E. J. Corey on the occasion of his 90th birthday.

Abstract: Macrophage migration inhibitory factor (MIF) is a proinflammatory cytokine that is implicated in the regulation of inflammation, cell proliferation, and neurological disorders. MIF is also an enzyme that functions as a keto-enol tautomerase. Most potent MIF tautomerase inhibitors incorporate a phenol, which hydrogen bonds to Asn97 in the active site. Starting from a 113- μ M docking hit, we report results of structure-based and computer-aided design that have provided substituted pyrazoles as phenol alternatives with potencies of 60-70 nM. Crystal structures of complexes of MIF with the pyrazoles highlight the contributions of hydrogen bonding with Lys32 and Asn97, and aryl-aryl interactions with Tyr36, Tyr95, and Phe113 to the binding.

Human macrophage migration inhibitory factor (MIF) is a proinflammatory cytokine that is implicated in the pathogenesis of numerous inflammatory diseases,^[1] neurological disorders,^[2] and cancer.^[3] MIF is expressed in many cell types and its tissue distribution is wide-spread. Upon activation of cells such as macrophages, monocytes and T-cells, expression of MIF in turn activates release of inflammatory cytokines including interleukins, interferon, and TNF α . Complex signaling pathways are invoked when MIF binds to its membrane-bound receptors CD74 and CXCR4, leading to leukocyte chemotaxis, inflammatory response, and potential tissue damage.^[3] Strong correlation is observed between MIF expression and the severity of many inflammatory and autoimmune diseases including asthma, sepsis, lupus, and rheumatoid arthritis.^[4] For cancer, the AKT pathway may be activated by MIF binding causing suppression of apoptosis by inhibition of the normal action of BAD, BAX, and p53.^[3] However, MIF's role in cancer is multifaceted with undesirable effects also on cell proliferation, angiogenesis, and metastasis.^[3,4] MIF is over-expressed in most human cancer cells.^[5]

Interestingly, MIF also shows enzymatic activity as a keto-enol tautomerase. MIF is a toroid-shaped, trimeric protein consisting of 342 amino acid residues with three identical active sites occurring at the interfaces of the monomer subunits.^[6] The active sites are small, relatively cylindrical and open to the surface

of the protein in the vicinity of Pro1, which serves as the catalytic base. The resultant strategy for interference with the binding of MIF to its receptor CD74 is then to find tautomerase inhibitors that change the surface characteristics of MIF.^[6] Indeed, numerous studies have shown a correlation between inhibition of the enzymatic and biological activities of MIF by measuring tautomerase activity, and, for example, MIF/CD74 binding, protein phosphorylation in inflamed cells, production of interleukins, and glucocorticoid overriding ability.^[6,7] Though many MIF tautomerase inhibitors have been discovered through screening of compound libraries,^[6,8] lead optimization to give inhibitors with nanomolar potency has been limited. In fact we have tested the most promising compounds from the literature in a tautomerase inhibition assay^[9] and only found compounds from one patent^[10] and our biaryltriazole series^[11] to have sub-micromolar K_i values. The results were confirmed by measurement of K_d values in a fluorescence polarization assay.^[12] Exemplary potent compounds are **1** (NVS-2^[10]) and **2**^[11] with K_i values of ca. 0.03 μ M, which are ca. 1000-fold lower than for well-known MIF inhibitors such as **3** ((*R*)-ISO-1^[13]) and the chromen-4-one **4**^[6a] (Scheme 1).



Scheme 1. Examples of MIF tautomerase inhibitors with K_i data from Ref. 12.

A feature, which is addressed here, is that **1** - **4** and many other non-covalent MIF tautomerase inhibitors and substrates contain a phenol subunit, which lodges in the back of the active site and forms hydrogen bonds with the sidechain of Asn97 (Figure 1).^[6,11,12] Though there are more than 125 approved drugs that contain a phenolic group including, for example, acetaminophen, albuterol, amoxicillin, raloxifene, and doxycycline, the oral bioavailability of phenols is well-known to often be unacceptably low owing to metabolic glucuronidation^[14] and/or sulfation.^[15] Thus, we set out to find a phenol-free series of MIF tautomerase inhibitors with low-nanomolar potencies.

Success in the past has come from exchange of the phenol for a 6:5 fused heteroaromatic incorporating a pyrrole or pyrazole that retains the hydrogen-bond donating character of phenol.^[16] However, the MIF active site is too constricted near Asn97 for this approach to be viable; addition of a methyl group *ortho* to the

[*] V. Trivedi-Parmar, Dr. M. J. Robertson, Dr. J. A. Cisneros, Dr. S. G. Krimmer, Prof. Dr. W. L. Jorgensen
Department of Chemistry
Yale University
New Haven, CT 06520-8107 (USA)

Prof. Dr. W. L. Jorgensen
E-mail: william.jorgensen@yale.edu

Supporting information for this article is given via a link at the end of the document.

COMMUNICATION

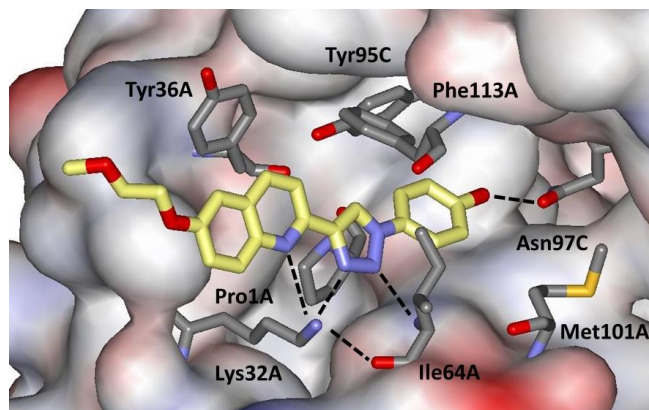
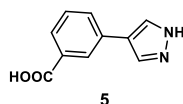


Figure 1. Rendering from a 1.8-Å crystal structure of an analog of **2** bound to MIF.^[11a] Carbon atoms of the inhibitor are colored yellow. Hydrogen bonds are indicated with dashed lines.

hydroxyl group for the compound in Figure 1 leads to a ca. 100-fold loss in activity.^[11a] Instead, our interest has focused on replacement of the phenol by a pyrazole. Owing to the geometrical differences, this requires exploration of new series with a pyrazole core. Fortunately, in the initial virtual screening study^[8a] 11 compounds were found to be active in an assay that measured interference of binding between MIF and immobilized CD74 ectodomain; and, one contained a pyrazole with the expected hydrogen bonds to Asn97 in the docked structure. This compound, **5**, gave an IC_{50} of 15 μ M in the binding assay; how-



Scheme 2. Docking hit **5**.^[8a]

ever, it showed little activity in a tautomerase assay using 4-hydroxyphenylpyruvate (HPP) as the substrate, with a maximum of 30% inhibition at 50 μ M.^[8a] Thus, we pursued alternative series from the virtual screening and from *de novo* design, which provided the biaryltriazoles including **2**.^[11] However, our interest in **5** was renewed since in another phenol-containing inhibitor series^[8b] rapid metabolic glucuronidation and sulfation were observed. It was decided to retest **5** in an HPP tautomerase assay using optimized protocols in our laboratory.^[9] Though the K_i for **5** from this assay was only 113 μ M, in view of its low molecular weight and possibilities for substitution in the phenyl ring, we were encouraged to perform structure-based, computer-aided lead optimization.^[17] As detailed here, this has been successful in providing pyrazole derivatives with ca. 2000-fold greater potency.

In working with **5**, it was noted that it had high solubility in polar media. This motivated successful pursuit of a crystal structure with MIF in spite of the modest K_i (Figure 2). There are two copies of **5** in each MIF trimer. The expected hydrogen bonds with Asn97 have average N-O and N-N lengths of 3.0 and 3.1 Å, while Lys32 has hydrogen bonds with the carboxylate group of **5** (3.0 and 2.7 Å) and the oxygen atom of Ile64 (2.7 Å). The NH of Ile64 also forms one with the carboxylate (2.9 Å), and the phenyl ring of **5** is well packed between Pro1, Tyr95, and Phe113. From this structure and model building with the BOMB program,^[17b]

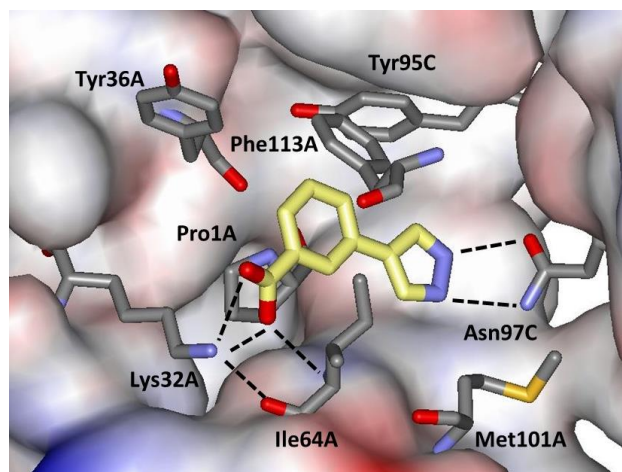
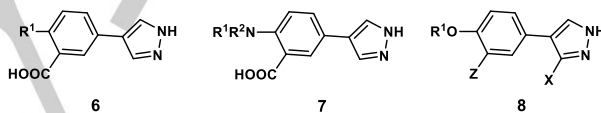


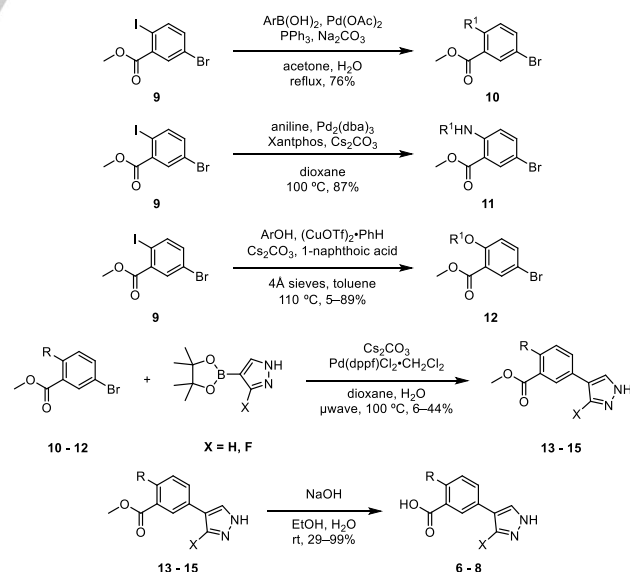
Figure 2. Rendering from the 2.0-Å crystal structure of **5** bound to MIF. Details as in Figure 1.

substitution *para* to the pyrazolyl group seemed likely to yield beneficial interactions with Tyr36 and possibly Phe113. Thus, constructs **6** – **8** were pursued where R^1 was mostly an aryl group.



Scheme 3. Designs for pyrazole-based MIF inhibitors.

The syntheses of **6** – **8** are detailed in the Supplementary Information. As summarized in Scheme 4, the key steps started from the commercially available phenyl iodide **9**, which underwent Pd- or Cu-mediated coupling to yield phenylaryl, arylaniliny, or biaryl ether derivatives **10** – **12**. Installation of the pyrazole was then achieved by a Suzuki coupling to yield esters **13** – **15**, which were hydrolyzed under mild conditions to provide the desired carboxylic acids.



Scheme 4. Synthesis of pyrazole-based MIF inhibitors.

COMMUNICATION

The compounds reported here are listed in Table 1 along with the results from the tautomerase assay. The identity of assayed compounds was confirmed by ^1H and ^{13}C NMR and high-resolution mass spectrometry; HPLC analyses established purity as >95%. As in prior studies, the inhibition constants K_i were determined using HPP as the substrate.^[9,11] Inhibitory activity is

Table 1. Experimental inhibition constants, K_i

Cmpd	R ^{1[a]}	R ²	Z	X	K_i (μM)
5	H	-	-	-	113
6a	Ph	-	-	-	20.6
6b	1-Np	-	-	-	19.5
6c	2-Np	-	-	-	5.4
7a	Ph	H	-	-	12.7
7b	2-Np	Me	-	-	4.2
8a	Ph	-	COOH	H	6.8
8b	<i>o</i> -MePh	-	COOH	H	4.3
8c	<i>m</i> -MePh	-	COOH	H	3.8
8d	<i>p</i> -MePh	-	COOH	H	7.0
8e	<i>m</i> -FPh	-	COOH	H	1.7
8f	<i>p</i> -FPh	-	COOH	H	4.6
8g	2-Np	-	COOH	H	4.3
8h	2-Np	-	SO ₂ Me	H	6.4
8i	2-Np	-	SO ₂ NH ₂	H	5.6
8j	9-Phenanthryl	-	COOH	H	2.3
8k	2-Adamantyl	-	COOH	H	2.6
8l	4-Acen	-	COOH	H	1.1
8m	1-Np	-	COOH	F	0.48
8n	2-Np	-	COOH	F	0.51
8o	4-Et-2-Np	-	COOH	F	0.15
8p	5-Et-2-Np	-	COOH	F	0.17
8q	7-Et-2-Np	-	COOH	F	0.14
8r	4-Cp-2-Np	-	COOH	F	0.11
8s	4-Cp,7-Et-2-Np	-	COOH	F	0.066
8t	<i>p</i> -Bp	-	COOH	F	0.35
8u	<i>m</i> -Bp	-	COOH	F	0.13
8v	3,5-diMe- <i>m</i> -Bp	-	COOH	F	0.24
8w	4-OEt- <i>m</i> -Bp	-	COOH	F	0.075
8x	4-MrPrO- <i>m</i> -Bp	-	COOH	F	0.067

[a] Np = naphthyl; Acen = 1,2-dihydroacenaphthyl; Cp = cyclopropyl; Bp = biphenyl; MrPrO = *N*-morpholinylpropoxy.

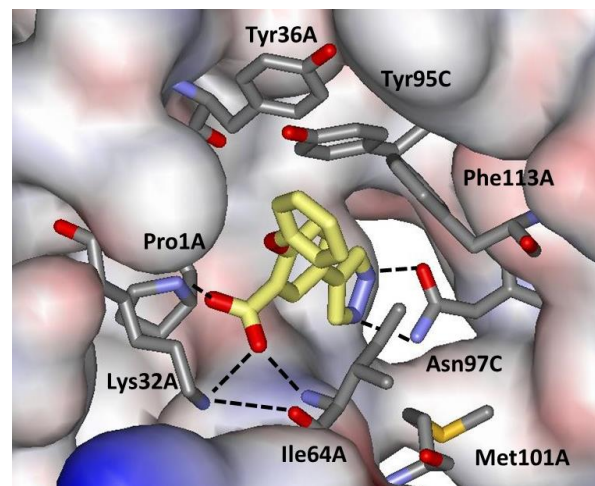


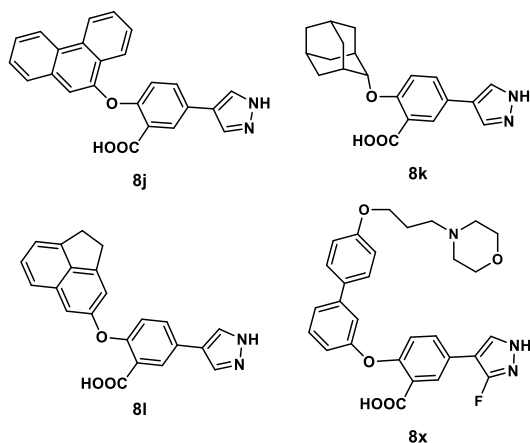
Figure 3. Rendering from the 2.3-Å crystal structure of **8a** bound to MIF. Details as in Figure 1.

measured from formation of the borate complex of the enol product at 305 nm using a plate reader. Absorbance is measured in triplicate on two occasions. The average K_i results are reported; the standard error is typically 10-20% of the K_i value. In addition, the aqueous solubilities of several compounds were determined with a shake-flask procedure.^[11,12,18] Saturated solutions are filtered and analyzed by UV-vis spectroscopy.

Consistent with the modeling, addition of an aryl group in **6** did provide a significant boost over **5**, bringing the K_i values down to ca. 20 μM for a phenyl or 1-naphthyl group and to 5 μM for 2-naphthyl (**6c**). The analogous aniliny and phenoxy compounds, **7a** and **8a**, were prepared, and the greater activity and pharmacological desirability of diarylethers placed the subsequent focus on the latter series. A 2.3-Å crystal structure for the complex of **8a** with MIF was also obtained (Figure 3), which does show aryl-aryl contacts between the phenoxy phenyl group and both Tyr36 and Phe113. A basic SAR (structure-activity relationship) study was then carried out with **8b** – **8f**, which revealed a small activity range for addition of a methyl or fluoro substituent, with *para*-substitution the least favored. Consistent with this guidance, the 2-naphthyl analog **8g** was found to show good activity at 4.3 μM ; the BOMB modeling indicated increased contact with Phe113 projecting to the right in Figure 3. Modeling further indicated that still larger hydrophobic groups could be accommodated in this region at the entrance of the MIF active site. This was borne out by K_i values of 1 - 3 μM obtained for phenanthryl, adamantyl, and acenaphthyl analogs, **8j** – **8l** (Scheme 5). However, the project seemed stalled at this point without reaching the desired low-nanomolar range and with increasing concerns about solubility.

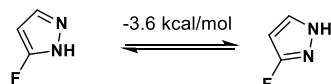
For the biaryltriazoles series, it was recalled that placement of a fluorine adjacent to the hydroxyl group in compounds like **2** provided a ca. 3-fold increase in activity.^[11] The effect was attributed to enhancing the acidity of the phenol, which increases the strength of the hydrogen bond with Asn97, and also to hydrophobic contact of the fluorine with the side chain of Met 101 (Figure 1). For the pyrazoles, the enhanced hydrogen bonding could be envisioned for a fluorine at the 3-position; however, the

COMMUNICATION



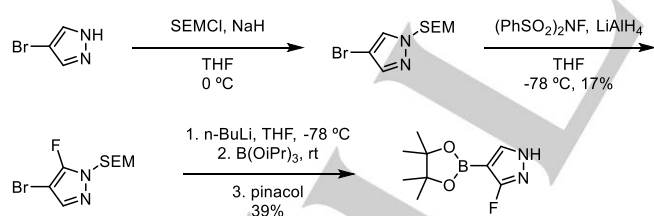
Scheme 5. Some pyrazole-based MIF inhibitors reported here.

fluorine would project more towards the side chain of Ile64 rather than Met101 with uncertain outcome (Figure 2). Still, a potential additional benefit might arise from the influence of the fluorine on the tautomeric equilibrium for the pyrazole. Reliable quantum mechanical calculations (MP2/6-311++G**) show that the N1-H tautomer is favored by 3.6 kcal/mol over the N2-H tautomer with a fluorine in the 3-position (Scheme 6).^[19] From the present crystal structures the hydrogen bonds are expected to be more linear for the N1-H tautomer as implied by the alignment of the side-chain oxygen atom of Asn97 and N1 in Figures 2 and 3.



Scheme 6. Shift in the tautomeric equilibrium with a fluorine.^[19]

Preparation of the fluorinated pyrazole for the Suzuki coupling in Scheme 3 proved difficult. Multiple routes were attempted, but success was only achieved using a SEM [2-(trimethylsilyl)ethoxymethyl] protecting group; the yield was still low, but sufficient to proceed (Scheme 7).



Scheme 7. Synthesis of fluorinated pyrazoles.

The effort was highly fruitful yielding a nearly 10-fold increase in potency in progressing from the parent 2-naphthyl inhibitor **8g** (4.3 μM) to its fluorinated analog **8n** (0.51 μM). It was also possible to obtain a crystal structure for this compound in complex with MIF at 2.0-Å resolution (Figure 4). The structure confirmed the positioning of the fluorine between the sidechains of Ile64 and Met101. There is one copy of the inhibitor in each MIF trimer in this case; the N-O and N-N hydrogen bond lengths with Asn97 are 2.87 and 3.12 Å. There are also close-packed

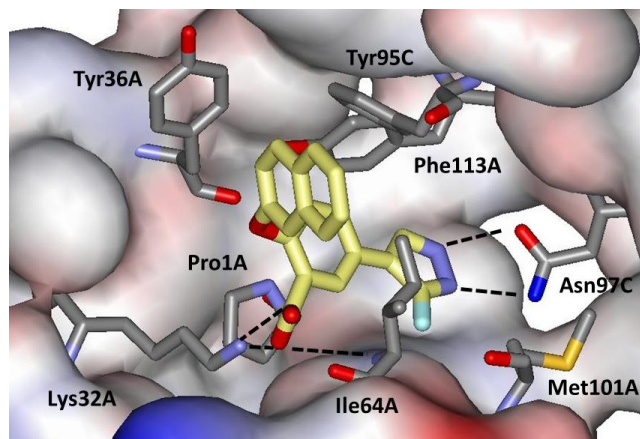


Figure 4. Rendering from the 2.0-Å crystal structure of **8n** bound to MIF. Details as in Figure 1.

aryl-aryl interactions between the naphthyl group of **8n** and Tyr36 and Phe113.

Though the exact positioning of the naphthyl group may be influenced by crystal packing, the structure and BOMB modeling indicated that additional gains in activity could arise from alkyl-substitution at the 4-, and 5-positions of the naphthyl group to achieve further contact with Phe113 or at the 7-position for contact with Ile64. This was shown to be correct with the ethyl analogs **8o**, **8p**, and **8q**, which each provided a 3-fold lowering of the K_i relative to **8n**. Addition of a cyclopropyl group at the 4-position also appeared promising for interaction with the front edge of Phe113; this was realized with **8r** bringing the K_i to 0.11 μM . Combining this with the 7-ethyl substitution provided the very potent **8s** with a K_i of 0.066 μM . From the structures for **8a** and **8n** (Figures 3 and 4) and modeling, it was also clear that it should be possible to expand to a biphenyl at either the *para* or *meta* position of **8a**. Thus, **8t** and **8u** were synthesized and provided significantly lower K_i values (0.35 and 0.13 μM) than the unsubstituted naphthyl analogs, **8m** and **8n**. Substantial activity gains could be expected by judicious substitution for the biphenyls; however, only a few derivatives were prepared with **8w** and **8x** (Scheme 4) demonstrating ca. 0.07 μM potency and that large groups can be extended into the solvent from the terminal 4-position.

Two additional items are worth noting. First, the results for **8g**, **8h**, and **8i** show that the carboxylic acid group may be replaced by a methylsulfone or sulfonamide with little impact on potency. This is relevant if one wished to explore these compounds as potential neurological agents,^[2] since sulfones are expected to exhibit better penetration of the blood-brain barrier than carboxylic acids or sulfonamides.^[20] Secondly, it is always important to monitor aqueous solubilities for compounds of interest for oral administration.^[11,17,21] Most oral drugs are observed to have aqueous solubilities of 4 to 4000 $\mu\text{g/mL}$, which translates to 10 μM to 10 mM for a drug with a molecular weight of 400.^[21] The solubilities of several of the present compounds were measured in Britton-Robinson buffer at pH 6.5.^[18] As noted, the solubility of the starting compound **5** is very high (927 \pm 88 $\mu\text{g/mL}$). The solubility of the parent 2-naphthyl analog **8g** is also high (739 \pm 32 $\mu\text{g/mL}$); it is affected little by addition of the fluorine in **8n** (681 \pm 59 $\mu\text{g/mL}$), while switch to the sulfonamide **8i** yields

COMMUNICATION

a significant reduction ($55.2 \pm 4.8 \mu\text{g/mL}$). Given these results, it was surprising to find in the biphenyl series that the solubility of **8w** is only $1.7 \pm 0.7 \mu\text{g/mL}$. However, this is readily remedied by attachment of solvent-exposed, solubilizing groups^[11b] as in **8x** ($34.6 \pm 4.8 \mu\text{g/mL}$, or $67 \mu\text{M}$).

In order to facilitate further study of the *in vitro* and *in vivo* biology of MIF, series of potent MIF tautomerase inhibitors have been pursued. Starting from a $113\text{-}\mu\text{M}$ docking hit, a novel series, which features a pyrazole instead of a phenol, was optimized to yield compounds with K_i values as low as $60\text{-}70 \text{ nM}$. The optimization was greatly facilitated by molecular modeling and the ability to obtain multiple high-resolution crystal structures, which guided the effective selection and placement of substituents. Recognition of the potential benefit of addition of a fluorine in the pyrazole ring also provided an essential boost along with a synthetic challenge. Current efforts are being directed at testing the influence of the inhibitors on suppressing MIF-stimulated cell proliferation and at preclinical studies for off-target activity and metabolism.

Experimental Section

Recombinant expression and purification of human MIF was carried out as previously reported.^[11] Crystallization of MIF in complex with **5** and **8g** was achieved by soaking with apo-MIF crystals, while for the complexes of **8a** and **8n**, co-crystallization was performed via sitting drop vapor diffusion at 20°C . The structures were determined in-house using a Rigaku 007 HF+ diffractometer and Saturn 944+ CCD detector at $T = 100 \text{ K}$. The crystal structures have been deposited in the RSC Protein Data Bank with IDs 6CBG (**5**), 6CBF (**8a**), 6CB5 (**8g**), and 6CBH (**8n**). The Supporting Information contains the synthetic procedures, NMR and HRMS spectral data for all new compounds, and details for the crystallography and solubility measurements (72 pages).

Acknowledgements

Gratitude is expressed to the U. S. National Institutes of Health (GM32136) for research support, to the National Science Foundation for a fellowship for MJR (DGE-1122492), and to Drs. Thomas Steitz, Michael Strickler, and Yong Xiong for assistance at the Yale Richards Center.

Conflict of interest

The authors declare no conflict of interest.

Keywords: MIF inhibitors • pyrazole • phenol bioisostere • tautomerase • protein crystallography

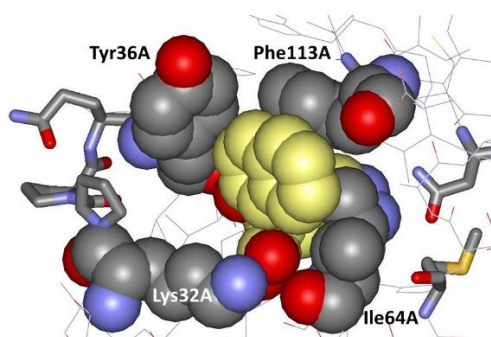
- [1] a) E. Lolis, R. Bucala, *Expert Opin. Ther. Targets* **2003**, *7*, 153-164. b) J. Garai, T. Lóránd, *Curr. Med. Chem.* **2009**, *16*, 1091-1114. c) D. Greven, L. Leng, R. Bucala, *Expert Opin. Ther. Targets* **2010**, *14*, 253-264; d) Y. Asare, M. Schmitt, J. Bernhagen, *Thromb. Haemost.* **2013**, *109*, 391-398.
- [2] a) N. E. Savaskan, G. Fingerle-Rowson, M. Buchfelder, I. Y. Eyüpoglu, *Int. J. Cell Biol.* **2012**, *2012*, 139573. b) M. F. Leyton-James, J. Kahn, A. Israelson, *Exp. Neurol.* **2018**, *301B*, 83-91.
- [3] a) C. Bifulco, K. McDaniel, L. Leng, R. Bucala, *Curr. Pharm. Design* **2008**, *14*, 3790-3801. b) H. Conroy, L. Mawhinney, S. C. Donnelly, *Q. J. Med.* **2010**, *103*, 831-836; c) L. Pawig, C. Klasen, C. Weber, J. Bernhagen, H. Noels, *Front. Immunol.* **2015**, *6*, 429. d) N. Kindt, F. Journe, G. Laurent, S. Saussez, *Oncol. Lett.* **2016**, *12*, 2247-2253. e) C. C. G. Nobre, J. M. Galvão de Araújo, T. A. A. M. Fernandes, R. N. O. Cobucci, D. C. F. Lanza, V. S. Andrade, J. V. Fernandes, *Pathol. Oncol. Res.* **2017**, *23*, 235-244.
- [4] C. O'Reilly, M. Doroudian, L. Mawhinney, S. C. Donnelly, *Med. Res. Rev.* **2016**, *36*, 440-460.
- [5] S. N. Babu, G. Chetal, S. Kumar *Asian Pac. J. Cancer Prev.* **2012**, *13*, 1737-1744.
- [6] a) M. Orita, S. Yamamoto, N. Katayama, S. Fujita, *Curr. Pharm. Design* **2002**, *8*, 1297-1317; b) J. Garai, T. Lóránd, *Curr. Med. Chem.* **2009**, *16*, 1091-1114; c) J. Bloom, S. Sun, Y. Al-Abed, *Expert Opin. Ther. Targets* **2016**, *20*, 1463-1475.
- [7] a) P. D. Senter, Y. Al-Abed, C. N. Metz, F. Benigni, R. A. Mitchell, J. Chesney, J. Han, C. G. Gartner, S. D. Nelson, G. J. Todaro, R. Bucala, *Proc. Natl. Acad. Sci. U.S.A.* **2002**, *99*, 144-149; b) A. A. Hare, L. Leng, S. Gandavadi, X. Du, Z. Courmia, R. Bucala, W. L. Jorgensen, *Bioorg. Med. Chem. Lett.* **2010**, *20*, 5811-5814.
- [8] a) Z. Courmia, L. Leng, S. Gandavadi, X. Du, R. Bucala, W. L. Jorgensen, *J. Med. Chem.* **2009**, *52*, 416-424; b) H. Ouertatani-Sakouhi, F. El-Turk, B. Fauvet, M.-K. Cho, D. P. Karpinar, D. Le Roy, M. Dewor, T. Roger, J. Bernhagen, T. Calandra, M. Zwickstetter, H. A. Lashuel, *J. Biol. Chem.* **2010**, *285*, 26581-26598; c) L. Xu, Y. Zhang, L. Zheng, C. Qiao, Y. Li, D. Li, X. Zhen, T. Hou, T. J. Med. Chem. **2014**, *57*, 3737-3745; d) L.-T. Tsai, T.-H. Lin, *J. Biomol. Screen.* **2014**, *19*, 1116-1123; e) M. C. Zapatero, P. Pérez, M. J. Vázquez, G. Colmenarejo, M. de los Frailes, F. Ramón, *J. Biomol. Screen.* **2016**, *21*, 1-13.
- [9] J. A. Cisneros, M. J. Robertson, M. Valhondo, W. L. Jorgensen, *Bioorg. Med. Chem. Lett.* **2016**, *26*, 2764-2767.
- [10] A. Billich, P. Lehr, H. Gstach, PCT/EP2005/011233, WO2006/045505 A1, **2006**.
- [11] a) P. Dziedzic, J. A. Cisneros, M. J. Robertson, A. A. Hare, N. E. Danford, R. H. Baxter, W. L. Jorgensen, W. L. J. Am. Chem. Soc. **2015**, *137*, 2996-3003; b) J. A. Cisneros, M. J. Robertson, B. Q. Mercado, W. L. Jorgensen, *ACS Med. Chem. Lett.* **2017**, *8*, 124-127.
- [12] J. A. Cisneros, M. J. Robertson, M. Valhondo, W. L. Jorgensen, *J. Am. Chem. Soc.* **2016**, *138*, 8630-8638.
- [13] Y. Al-Abed, D. Dabideen, B. Aljabari, A. Valster, D. Messmer, M. Ochani, R. H. Baxter, K. Ochani, M. Bacher, F. Nicoletti, C. Metz, V. A. Pavlov, E. J. Miller, K. J. Tracey, *J. Biol. Chem.* **2005**, *280*, 36541-36544.
- [14] a) B. Wu, K. Kulkarni, S. Basu, S. Zhang, M. Hu, *J. Pharm. Sci.* **2011**, *100*, 3655-3681; b) A. Rowland, J. O. Miners, P. I. Mackenzie, *Int. J. Biochem. Cell Biol.* **2011**, *45*, 1121-1132.
- [15] a) E. Chapman, M. D. Best, S. R. Hanson, C.-H. Wong, *Angew. Chem. Int. Ed.* **2004**, *43*, 3526-3548; b) C. Rakers, F. Schumacher, W. Meinel, H. Glatt, B. Kleuser, G. Wolber, *J. Biol. Chem.* **2016**, *291*, 58-71.
- [16] a) J. L. Wright, T. F. Gregory, S. R. Kesten, P. A. Boxer, K. A. Serpa, L. T. Meltzer, L. D. Wise, *J. Med. Chem.* **2000**, *43*, 3408-3419; b) R. R. Wilkening, R. W. Ratcliffe, A. K. Fried, D. Meng, W. Sun, L. Colwell, S. Lambert, M. Greenlee, S. Nilsson, A. Thorsell, M. Mojena, C. Tudela, K. Frisch, W. Chan, E. T. Birzin, S. P. Rohrer, M. L. Hammond, *Bioorg. Med. Chem. Lett.* **2006**, *16*, 3896-3901.
- [17] a) H. Gohlke, G. Klebe, *Angew. Chem. Int. Ed. Engl.* **2002**, *41*, 2644; b) W. L. Jorgensen, *Acc. Chem. Res.* **2009**, *42*, 724-733; c) P. Schneider, G. Schneider, *J. Med. Chem.* **2016**, *59*, 4077-4086; d) W. L. Jorgensen, *Bioorg. Med. Chem.* **2016**, *24*, 4768-4778.
- [18] E. Baka, J. E. A. Comer, K. Takács-Novák, *J. Pharm. Biomed. Anal.* **2008**, *46*, 335-341.
- [19] M. Jarończyk, J. C. Dobrowolski, A. P. Maruzek, *J. Mol. Struct. (Theochem)* **2004**, *673*, 17-28.
- [20] a) S. A. Hitchcock, L. D. Pennington, *J. Med. Chem.* **2006**, *49*, 7559-7583; b) J. M. Meinig, S. J. Ferrara, T. Banerji, T. Banerji, H. S. Sanford-Crane, D. Bourdette, T. S. Scanlan, *ACS Chem. Neurosci.* **2017**, *8*, 2468-2476.
- [21] W. L. Jorgensen, E. M. Duffy, *Adv. Drug Deliv. Rev.* **2002**, *54*, 355-366.

COMMUNICATION

Entry for the Table of Contents

COMMUNICATION

A novel inhibitor series has been pursued for macrophage migration inhibitory factor (MIF). Starting from a 113- μ M docking hit, results of structure-based and computer-aided design are reported to yield substituted pyrazoles as alternatives to metabolically labile phenols with potencies of 60-70 nM.



*Vinay Trivedi-Parmar, Michael J. Robertson, José A. Cisneros, Stefan G. Krimmer, and William L. Jorgensen**

Page No. – Page No.

Optimization of Pyrazoles as Phenol Surrogates to Yield Potent Inhibitors of Macrophage Migration Inhibitory Factor